Microstructure of segmented amorphous polyurethanes: small-angle X-ray scattering and mechanical spectroscopy studies

S. Etienne* and G. Vigier
Groupe d'Etudes de Métallurgie Physique et de Physique des Matériaux, UA CNRS 341, Institut National des Sciences Appliquées (INSA), bât. 502, 69621 Villeurbanne Cedex, France

and L. Cuvé and J. P. Pascault
Laboratoire des Matériaux Macromoléculaires, UA CNRS 507, Institut National des Sciences Appliquées (INSA), bât. 303, 69621 Villeurbanne Cedex, France
(Received 8 March 1993; revised 30 September 1993)

The microstructure of polyurethanes and its evolution upon thermal treatment were investigated by means of small-angle X-ray scattering and low-frequency high-resolution mechanical spectroscopy. The segmented copolymer materials studied in this work were prepared in bulk and were completely amorphous as a consequence of the chemical composition of the soft and hard segments. This amorphous state results in model materials and, in principle, easier interpretation of the morphology from experimental results. It is shown in this work that thermal treatment induces a coarsening of hard-phase microdomains and an increase of the interfacial region, which remains of the order of a few ångströms. This morphology evolution leads, to some extent, to a weakening of the mechanical properties as observed above the glass transition temperature of the soft-phase matrix. The conclusion is that the synthesis conditions, as well as subsequent heat treatment, are to be carefully considered in order to obtain materials with well controlled physical properties.

(Keywords: amorphous polyurethane; mechanical spectroscopy; small-angle X-ray scattering)

INTRODUCTION

Segmented polyurethanes are thermoplastic materials exhibiting an elastomeric behaviour at room temperature. Their unique physical properties and more particularly their dynamic mechanical behaviour are due to microphase separation, microdomains rich in hard segments acting as physical crosslinks. The two-phase microstructure is induced by the strong thermodynamic immiscibility between soft segments and polar hard segments.

Reliable microstructural investigation of segmented polyurethanes (PU), and more generally of block copolymers, requires a great number of experimental characterizations. Since the early studies of Wilkes *et al.*[1,2], a lot of work using different techniques (small-angle X-ray scattering (SAXS), differential scanning calorimetry (d.s.c.), transmission electron microscopy, mechanical and dielectric spectroscopies, nuclear magnetic resonance (n.m.r.)) have been devoted to the investigation of the morphology and its influence on the physical properties of these materials (see for instance refs 3 to 12).

The aim of this work is to study the microstructure of segmented polyurethanes, and its evolution, by SAXS and to analyse the micromechanical properties linked to this microstructure. In order to avoid microstructural changes arising from crystallization, the polyurethanes considered here were synthesized with polyolefin soft segments (hydrogenated polybutadiene (HPBD)), which are amorphous and non-polar. The amorphous nature of the hard segments was achieved by using neopentyl glycol (NPG) as chain extender. The prepared materials exhibit microphase separation that is not always in thermodynamic equilibrium, as a consequence of the slowing down of diffusion-dominated processes during synthesis[13]. Thus, we have studied on the one hand the effect of high-temperature thermal treatments and on the other hand the kinetic aspects of the microstructural evolution by means of *in situ* SAXS experiments. The measurements of dynamic shear modulus were carried out by means of low-frequency mechanical spectroscopy and show relaxation effects that are sensitive to heat treatment. These results will be discussed and compared to those obtained by dielectric spectroscopy[13].

In this paper, the abbreviations H or S will be used to refer to the hard or soft segments, respectively.

EXPERIMENTAL

The material: synthesis and characterization

The starting reagents used for synthesis are reported in *Table 1*. The segmented polyurethanes with formulation:

$$-[\mathrm{HPBD}-((x-1)\mathrm{NPG}, x\mathrm{MDI})]-$$

were prepared following a two-step reaction.

*To whom correspondence should be addressed. Present address: LMPSM UACNRS 155, Ecole des Mines, Parc de Saurupt, 54042 Nancy Cedex, France

0032-3861/94/13/2737-07

Table 1 Characteristics of reagents

Segments	Reagents	Abbreviation	Formula	Supplier
Hard segments (HS)	Diisocyanate: 4,4′-methylene bis(*p*-phenyl isocyanate)	MDI	(1)	Bayer
	Chain extender: neopentyl glycol	NPG	(2)	BASF
Soft segments (SS)	α,ω-Hydroxy-terminated oligomer: hydrogenated polybutadiene	HPBD	(3)	Nippon Soda

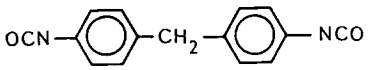

(1)

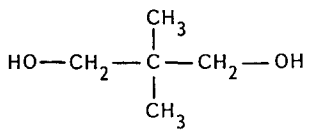

(2)

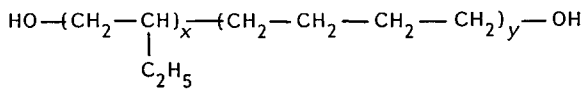

$x = 34,\ y = 4$

(3)

Table 2 Molecular weight as determined by s.e.c.

Polymer	Molar ratio HPBD/MDI/NPG	HS (wt%)	$\bar{M}_n$ (HS)	$\bar{M}_n$	$\bar{M}_w$
PU30	1/3/2	30	843	32800	107300
PU40	1/5/4	41	1540	26500	90400
PU50	1/7/6	50	2248	25900	76600

The synthesis procedure is described in detail elsewhere[13], so that only the main aspects are recalled here for convenience for the reader. First, the reaction takes place in bulk between 1 mol of macrodiol and an excess of x moles of diisocyanate at 80°C for 4 h in vacuum. At this stage, 200 ml of tetrahydrofuran (THF) are added at room temperature. Then, $x-1$ moles of chain extender and catalyst (0.01 wt% dibutyl dilaurate) are added and the reaction allowed to proceed for 3 h at 50°C. The polymer concentration in THF used as solvent reaches 10%. At the final step, the polymer is precipitated in methanol and dried in vacuum for 24 h at 60°C. Films are obtained from a solution of redissolved polymer in THF at room temperature. The PU thus prepared in solvent medium does not exhibit macrophase separation, which could be induced by the mutual immiscibility of the starting monomers. Furthermore, it is obtained in the amorphous state due to the nature of the soft segments (HPBD, rich in butene-1 radicals) and the hard segments (xMDI, $(x-1)$NPG), as quoted above. The microphase separation is expected to be well pronounced in this material because hydrogen bonds can form only between hard segments.

Three compositions were synthesized, which differ in hard-segment content. This variation in hard-segment amount was obtained by varying the x value, i.e. the length of hard segments. After synthesis of polymers, the molecular weights are determined by size exclusion chromatography. The formulations studied in this work are reported in *Table 2*.

Low-frequency mechanical spectrometry

The dynamic mechanical properties were measured by means of an inverted torsion pendulum working in the forced oscillations regime in the very-low-frequency range 10^{-5} to 10 Hz[14,15]. Experiments are carried out in vacuum and the temperature can be controlled and programmed in the range 77 to 500 K. The relative shear strain applied for the complex shear modulus measurement is maintained at a very low level and does not exceed 10^{-5}. After data processing, the apparatus gives directly the modulus as a function of angular frequency ω and/or temperature T: $G(i\omega) = G'(\omega) + iG''(\omega) = G(\omega)\exp[i\varphi(\omega)]$. The coefficient $\tan\varphi(\omega)$ is referred to as the loss factor.

Specimens suitable for mechanical spectroscopy experiments were prepared from the films and their dimensions were typically $2 \times 1 \times 10\,mm^3$.

Small-angle X-ray scattering

SAXS patterns were obtained by means of an assembly including: (i) a Rigaku Rotaflex generator with copper rotating anode; (ii) a point collimation block, the collimation being mainly obtained with two orthogonal mirrors presenting adjustable bending; (iii) a line position-sensitive detector with 512 channels, and 100 μm width

per channel; (iv) a multichannel analyser connected to a microcomputer for data collection and processing.

The sample is placed within a cell that allows one to perform *in situ* experiments at controlled temperature in the range 100 to 550 K.

The sample–detector distance allows one to adjust the angular domain under investigation. In the frame of this study, the 2θ angular domain extends from 1 mrad up to 60 mrad. Thus, the corresponding size of microdomains that can be studied extends to about 100 nm.

RESULTS

First the characteristic temperatures of the specimens were measured by means of thermal analysis, then SAXS observations and mechanical spectroscopy experiments were carried out.

Thermal analysis

The glass transition temperatures were measured by d.s.c. (Mettler TA 3000). The results relative to the soft phase are reported in *Figure 1* and *Table 3* for the first (up to 240°C) and the second temperature scans.

It has been shown[16] that the ratio $\Delta C_{pS}/\Delta C_{p0}$ allows one to deduce the separation rate if ΔC_{p0} is the heat-capacity increment at the glass temperature of the soft phase T_{gS} for a pure soft phase and ΔC_{pS} the heat-capacity increment actually measured. Using this procedure, the phase separation rate was found to be about 85–88%[13]. This rather high value is in agreement with the high incompatibility between hard (polar) and soft (non-polar) segments as previously discussed. D.s.c. thermograms (first scan) reveal a transition near 32°C, which could be identified as the glass transition of the hard phase. The width of the transition increases as the molecular weight (i.e. polymolecularity) of hard segments increases, but the first stage of the endotherm is nearly constant. The low value of the glass transition temperature of the hard phase T_{gH} is attributed to the presence of soft segments in domains rich in hard segments. During the second scan, ΔC_{pH} decreases and ΔC_{pS} increases, as well as the temperature T_{gH}, suggesting that heat treatment up to 240°C at a heating rate of 7.5 K min^{-1} (which has occurred on the first temperature scan) enhances the phase separation.

Dynamic shear modulus

Isochronal (frequency = 0.3 Hz) curves, displayed on *Figures 2, 3* and *4*, obtained for each composition show the following features:

A secondary relaxation near 120 K is attributed to local motions of soft segments, since its strength is a decreasing function of the hard-segment content. The frequency dependence analysis yields the apparent activation energy 25 kJ mol^{-1} and a pre-exponential factor 10^{-10} s. A similar relaxation process was already observed in polytetramethylene soft-segment-based PU[17].

A relaxation near 250 K is associated with a drastic drop of the modulus over several decades in magnitude, and associated to the glass transition of the soft phase.

Above 270 K, the storage modulus G' exhibits a plateau, the level of which is an increasing function of the whole hard-segment content (see *Table 3*). In order to achieve reliable values of the plateau modulus, an extrapolation procedure of the isochronal plot $G''(G')$ was carried out, as shown on *Figure 5*. This plateau is followed

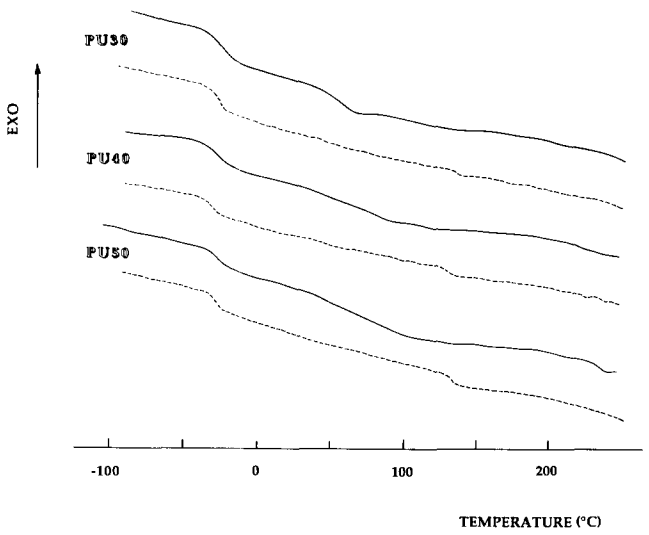

Figure 1 Thermograms exhibited by the three polyurethane samples during the first (—) and second (– – – –) scans

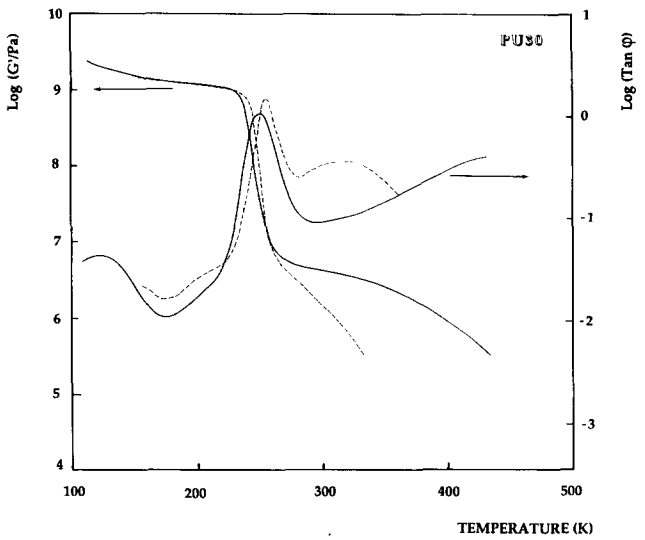

Figure 2 Dynamic shear modulus (frequency 0.3 Hz) of PU30 sample: (—) as-prepared material; (– – – –) after thermal treatment

Table 3 Thermal and mechanical properties

Polymer	First scan		Second scan		Plateau modulus, G' (MPa)
	T_{gS} (°C) (soft segments)	ΔC_{pS} (J g^{-1} K^{-1})	T_{gS} (°C) (soft segments)	ΔC_{pS} (J g^{-1} K^{-1})	
PU30	−35	0.22	−34	0.24	6.2
PU40	−34	0.20	−34	0.22	8
PU50	−34	0.17	−32	0.19	15

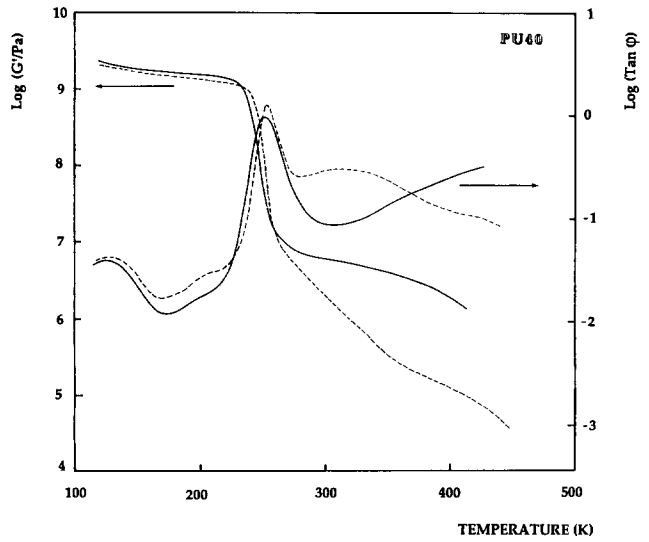

Figure 3 Dynamic shear modulus (frequency 0.3 Hz of PU40 sample: (—) as-prepared material; (– – – –) after thermal treatment

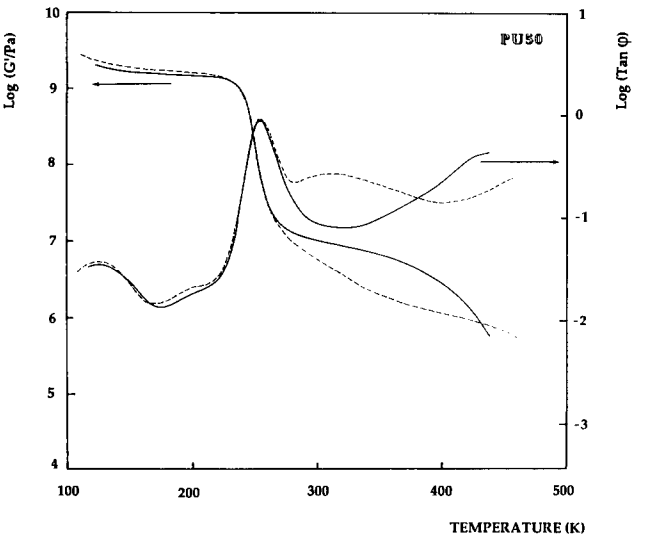

Figure 4 Dynamic shear modulus (frequency 0.3 Hz) of PU50 sample: (—) as-prepared material, (– – – –) after thermal treatment

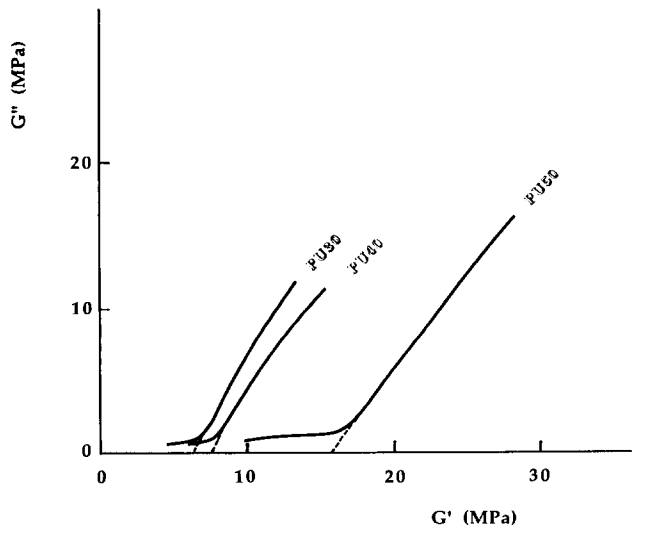

Figure 5 Cole–Cole diagram used to determine the plateau of the G' storage modulus observed above the main relaxation process due to the glassy transition of the soft phase

by a flow process at higher temperature, which manifests as a decrease of the storage modulus and a rise of tan φ loss coefficient. This flow process, starting from about 350 K, is attributed to a weakening of physical crosslinking, and could be associated with the main relaxation of microdomains rich in hard segments. Actually, this main mechanical relaxation, when measured at a frequency of the order of 1 Hz, occurs at a temperature not far from the calorimetric glass transition temperature[18].

After a thermal treatment above T_{gH} (150°C, 24 h), a drastic decreasing of mechanical properties can be observed at temperature higher than T_{gS} for the three compositions studied. Mainly, a relaxation process between 280 and 400 K leads to a high temperature dependence of the storage modulus in this temperature range instead of a plateau (see *Figures 2, 3* and *4*). Thus, it appears that the thermal treatment induces a weakening of the physical crosslinking as a consequence of a morphology change. We intend then in the following section to study in more detail and at a microscopic level the evolution of this morphology by SAXS experiments.

SAXS

Scattering patterns are shown on *Figure 6* for the three compositions after synthesis, i.e. before high-temperature treatment. In each case the pattern exhibits a well resolved correlation peak. The value of the scattering

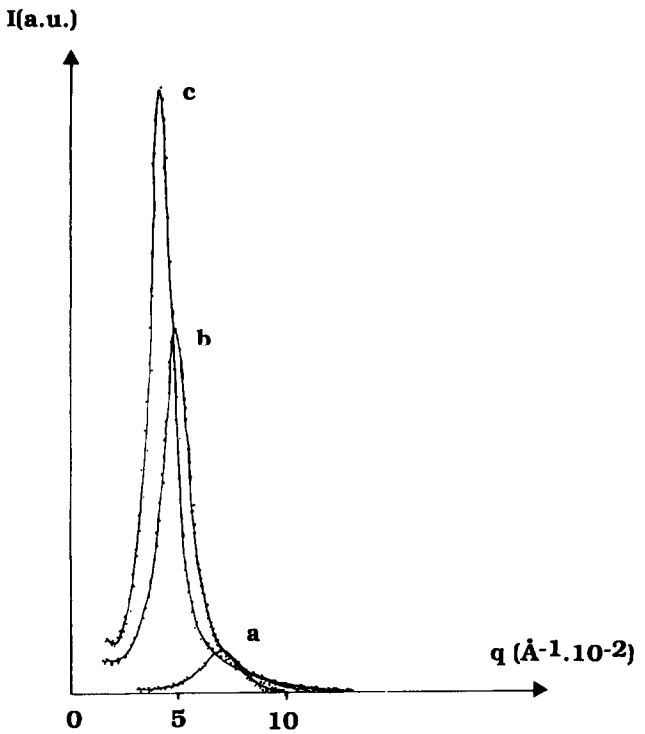

Figure 6 Scattering curves obtained for the three compositions: PU30 (curve a), PU40 (curve b) and PU50 (curve c); before thermal treatment

Table 4 SAXS results on as-prepared materials

Polymer	L_p (nm)	Q/P ratio (nm)
PU30	9.3	1.8
PU40	12.7	2.8
PU50	14.8	3.3

vector q corresponding to the peak decreases when the whole hard-segment ratio increases. The position of the peak on the q scale gives the correlation length, hereafter called the long period L_p, by simply considering the Bragg law. Assuming some hypothesis[19], the distance L_p is related to the distance between scattering particles. In the present study these particles are identified as microdomains rich in hard segments. As reported in *Table 4*, L_p increases as the content of hard segments increases.

The presence of a well pronounced correlation peak indicates a strong effect of interparticle interference on the scattering pattern. This effect prevented direct determination of the size of microdomains (e.g. the radius of gyration by Guinier's method) with confidence. However, this effect has no significant influence on the asymptotic behaviour of the scattering intensity at large values of the scattering vector q. This asymptotic behaviour is similar for the three compositions and obeys Porod's law to a good approximation: Porod's law is actually modified if a gradual interface between rigid domains and the soft matrix is present. As a matter of fact, the scattering intensity function $I(q)$ is often characterized by an asymptotic behaviour as:

$$I(q) = H(q)\frac{P}{q^4} + I_b$$

where I_b represents a background scattering term (mainly from thermal fluctuations), $H(q)$ is a function depending on the interface and P is the Porod constant. In the frame of this work, the q dependence of I_b can be neglected in the q range considered here and $H(q)$ is assumed to be written as[20]:

$$H(q) = 1 - \frac{e^2}{12}q^2$$

where e is the interface thickness, assuming a constant concentration gradient. The determination of e is not a simple task because it is highly dependent on the determination accuracy of the background I_b. Actually, a three-step procedure was carried out:

(i) Determination of the q_{min} value, where the asymptotic law seems to be obeyed, was the first step. To this end, the function $I(q)q^2$ is plotted against $1/q^2$ assuming I_b equal to zero. Doing so, a straight line is expected, the slope of which represents the Porod constant P and whose limit value at $1/q^2 = 0$ allows one to calculate the e value. Actually, the presence of the term I_b induces a curvature, mainly significant at low values of $1/q^2$. However, the q_{min} value is generally located without difficulty.

(ii) In a second step, the quantities P and I_b are determined using the least-squares fitting method between q_{min} and q_{max} (experimental limit of the scattering curve).

(iii) Finally, the effect of the background I_b is subtracted and the product $I(q)q^2$ is plotted again as a function of $1/q^2$ to check the validity of the procedure. An example of such data processing is given in *Figure 7*.

Low values of interface thickness, less than 0.5 nm, were found for the three compositions, with a tendency to increase with the hard-segment amount. Similar observations were already reported by Leung and Koberstein in the case of MDI–butanediol based polyurethanes[21]. However, these values are too small (actually, the data processing gives numerical values between 0 and 0.3 nm) to yield a definitive conclusion on the influence of hard-segment amount, and, in each case, the interface thickness can be considered as nearly negligible.

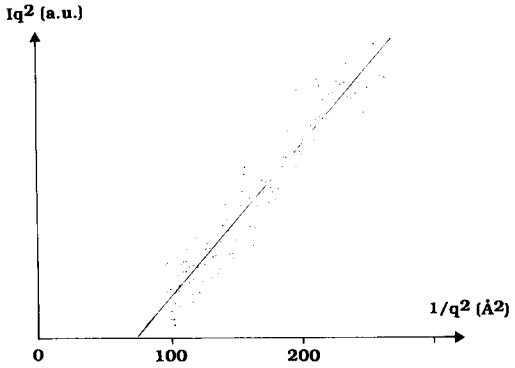

Figure 7 Asymptotic behaviour presented by a PU50 sample after 6 h at 155°C

The Q/P ratio, where Q is the integrated intensity, $Q = \int_0^\infty q^2 I(q)\,dq$, is nearly inversely proportional to the surface/volume ratio, i.e. proportional to the dimensions of scattering domains. The accuracy in the determination of this ratio is mainly dependent on the accuracy of the determination of P, which interferes also in the calculation of Q via the extrapolation of the experimental scattering curve between q_{max} and $q \to \infty$.

From the calculated values of the ratio Q/P we observe that the size of the scattering domains as well as the distance between them increase with the overall hard-segment content (see *Table 4*).

After studying the composition dependence, we have studied the effect of thermal treatment as a function of elapsed time. This treatment was carried out *in situ* at 155°C in the case of PU30 and PU50 and 165°C for PU40 and PU50 in the cell used for the scattering experiments. To this end, the sample is first heated from room temperature up to the treatment temperature at a rate 10 K min^{-1}. Then the temperature is kept constant within 1 K. The duration of exposure necessary for scattering data collection was about 600 s.

Figures 8, 9, 10 and *11* show the evolution against time of scattered intensity spectra presented by the samples PU30 and PU50 (at 155°C) and PU40 and PU50 (at 165°C) respectively. Four main features are to be reported:

(i) The scattering peak shifts towards lower values of q. This shift indicates an increasing long period L_p as represented on *Figure 12*. L_p determined from the 3d autocorrelation function yields qualitatively the same results, with slightly higher values however (about 15%).

(ii) The asymptotic behaviour obeys a $1/q^4$ law, eventually modulated by the interface effect.

(iii) The integrated intensity $\int_0^\infty q^2 I(q)\,dq$ remains nearly constant.

(v) The ratio Q/P increases in a way inversely proportional to the correlation length L_p. During the isothermal treatment, the quantity $(L_p P/Q)$ fluctuates around a mean value by less than 10%, i.e. remains nearly constant. The conclusion is that the microstructure remains self-similar but the characteristic length increases.

All these observations indicate that the main phenomenon occurring during these isothermal treatments at 155 and 165°C is the coarsening of microdomains. To

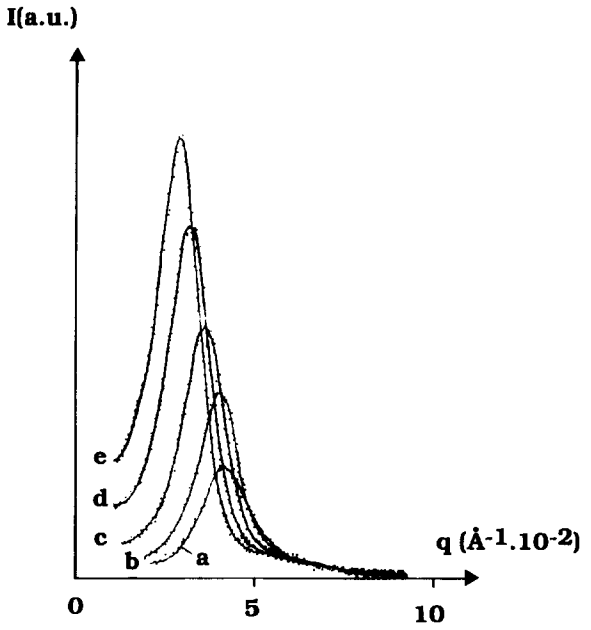

Figure 8 Evolution of the scattering curves of PU50 material during a thermal treatment at 155°C: before treatment (curve a); after treatment for 30, 120, 240 and 360 min (curves b, c, d and e respectively)

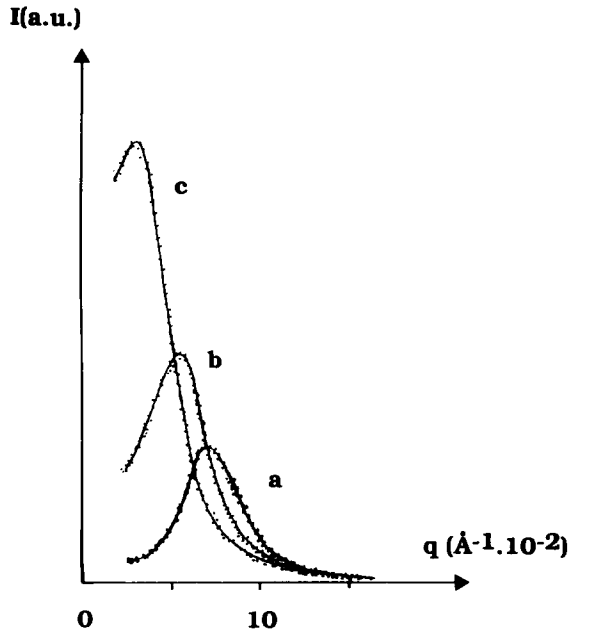

Figure 9 Evolution of the scattering curves of PU30 material during a thermal treatment at 155°C: before treatment (curve a); after treatment for 640 min (curve b) and 1200 min (curve c)

support this conclusion, we observe that L_p obeys to a good approximation a $t^{1/3}$ law, which is characteristic of coarsening phenomena[22,23] (*Figure 13*), at least in the first stages. In fact, the chemical linkage between hard and soft segments restricts the phase structure to the microscopic scale.

The thickness e of the interface, which is not simple to determine, remains very low in each case and can be neglected, as already quoted above. However, the data processing reveals its tendency to grow during thermal treatment, being the more important the higher the hard segments content: e is about 0.6 nm after 6 h at 155°C in the case of PU50, compared to 0.2 nm observed for PU30 in the same conditions.

Thermal treatments carried out at somewhat higher temperature yield similar effects, only the kinetics are faster.

DISCUSSION AND CONCLUSION

Small-angle X-ray experiments give evidence for a high microphase separation rate for the sequenced polyurethanes HPBD–(NPG, MDI). As the prepared materials were not heated above 60°C (i.e. a temperature below the glass transition temperature T_{gH} of the hard-segment phase) during their synthesis, it means that the phase segregation has not reached its equilibrium value (see figure 4 of ref. 13).

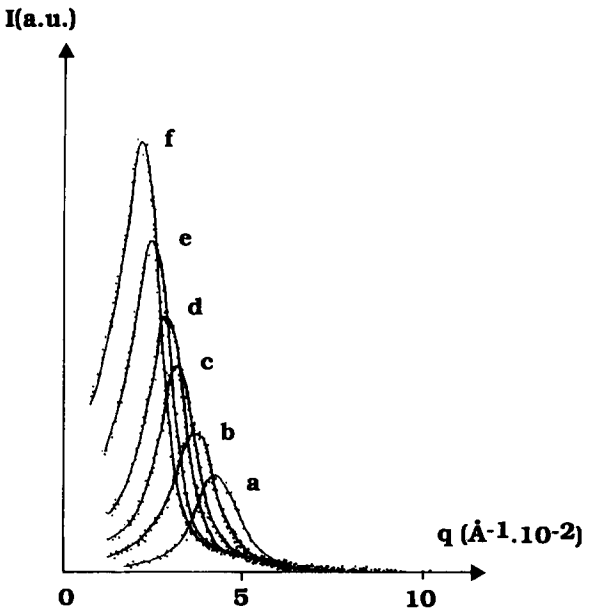

Figure 10 Evolution of the scattering curves of PU50 material during a thermal treatment at 165°C: before treatment (curve a); after treatment for 60, 120, 180, 300 and 420 min (curves b, c, d, e and f respectively)

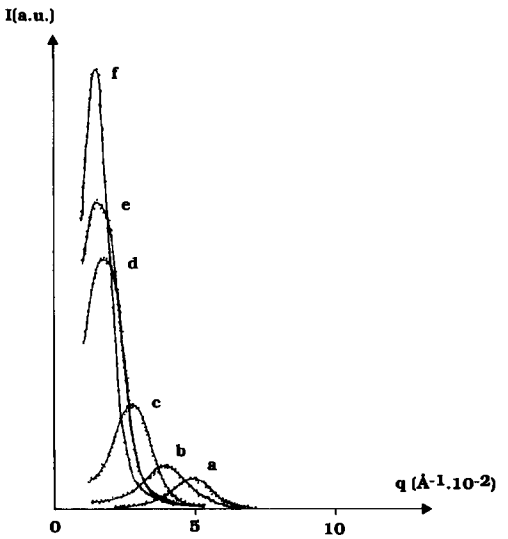

Figure 11 Evolution of the scattering curves of PU40 material during a thermal treatment at 165°C: before treatment (curve a); after treatment for 65, 240, 930, 1310 and 5340 min (curves b, c, d, e and f respectively)

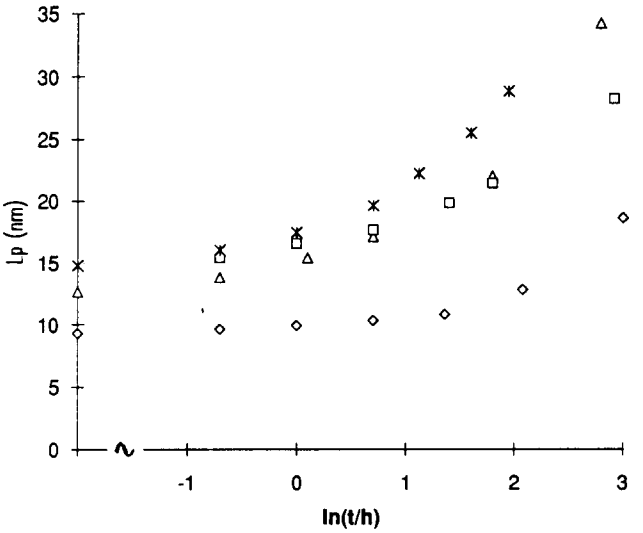

Figure 12 Evolution of the long period *versus* high-temperature treatment time: (◇) PU30, 155°C; (△) PU40, 165°C; (□) PU50, 155°C; (*) PU50, 165°C

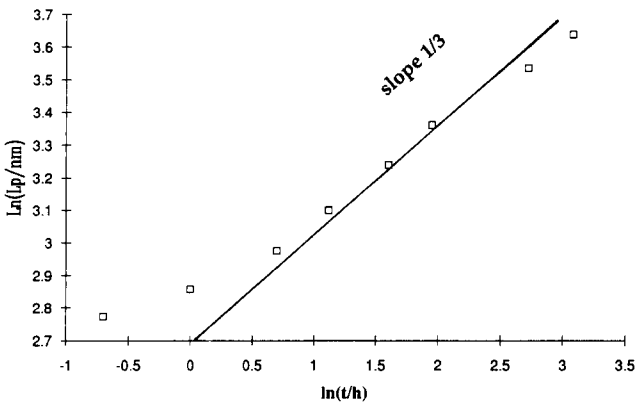

Figure 13 Evolution of the long period exhibited by a PU40 material *versus* time (logarithmic scale) at 165°C

Heat treatments carried out at 155 and at 165°C (i.e. at temperatures above T_{gH}) induce an evolution of the morphology. As a result, the size of hard-phase microdomains increases as well as their mean separation and the thickness of the gradual interface (or interphase). This interphase tends to increase when the hard-segment amount (i.e. their mean length and their distribution length) increases. The presence of hard segments in the interphase could explain the mechanical relaxation observed between 280 and 380 K at 1 Hz (see *Figures 2, 3* and *4*) after heat treatment. This observation is in agreement with the result of dielectric spectroscopy carried out on the same materials[13].

The point now is to estimate the mean path in the soft phase between two nearest domains. Considering, as a simple assumption, that the hard-segment domains are distributed on a cubic pseudo-lattice, this path is about 2 nm in the as-prepared materials and increases up to about 5 nm after heat treatment for the three compositions. This latter value is far below the end-to-end distance of soft segments in the stretched planar zig-zag configuration, but is higher than the r.m.s. end-to-end distance of soft segments, calculated to be about 2 nm from constrained-chains statistics[24]. The conclusion is that some isolated hard segments (mainly the shortest ones) dissolve in the soft matrix after heat treatments. These isolated hard segments could contribute to relaxations in addition to those included in the interphase.

It is worth noting that the coarsening process resulting from thermal treatments yields a degradation of elastomeric properties at temperatures above T_{gS}. Actually, physical crosslinking by small (but numerous) hard microdomains is more efficient than that produced by large (but less numerous) ones. This remark contrasts with the results of Bengston *et al.*[25], who observed that the mechanical properties of similar materials remained unaffected by heat treatments. Thus, heat treatments appear as a prominent parameter conditioning the physical properties.

Turning to the effect of the composition on the overall morphology, the existence of co-continuous phases in microphase-separated block copolymers is still questionable. The drop of shear modulus observed at T_{gS}, even in the case of specimens containing 50% of hard segments, shows clearly that such a situation does not occur in our materials.

REFERENCES

1 Wilkes, G. L. and Wildnauer, R. J. *J. Appl. Phys.* 1975, **46**, 4148
2 Ophir, Z. H. and Wilkes, G. L. *Adv. Ser. Chem.* 1979, **176**, 53
3 Koberstein, J. T. and Stein, R. S. *J. Polym. Sci., Polym. Phys. Edn.* 1983, **21**, 2181
4 Wang, C. B. and Cooper, S. L. *Macromolecules* 1983, **16**, 775
5 Yu, X.-H., Nagarajan, M. R., Grasel, T. G. and Gibson, P. E. *J. Polym. Sci., Polym. Phys. Edn.* 1985, **23**, 2310
6 Tyagi, D., McGrath, J. E. and Wilkes, G. L. *Polym. Eng. Sci.* 1986, **26**, 1371
7 Gibson, P. E., Van Bogart, J. W. C. and Cooper, S. L. *J. Polym. Sci. (B) Polym. Sci.* 1986, **24**, 885
8 Chen-Tsai, C. H. Y., Thomas, E. L., MacKnight, W. J. and Schneider, N. S. *Polymer* 1986, **27**, 659
9 Koberstein, J. T., Russell, T. J., Walsh, D. J. and Pottick, L. *Macromolecules* 1990, **23**, 877
10 Bates, F. S. and Fredrickson. G. H. *Annu. Rev. Phys. Chem.* 1990, **41**, 525
11 Koberstein, J. T., Yu, C. C., Galambos, A. F., Russell, T. P. and Ryan, A. J. *Polym. Prepr.* 1990, **31**, 110
12 Chu, B., Gao, T., Li, Y., Wang, J., Desper, C. R. and Byrne, C. A. *Macromolecules* 1992, **25**, 5724
13 Cuvé, L., Pascault, J. P., Boiteux, G. and Seytre, G. *Polymer* 1991, **32**, 343
14 Etienne, S., Cavaillé, J. Y., Perez, J., Point, R. and Salvia, M. *Rev. Sci. Instrum.* 1982, **53**, 1261
15 Etienne, S. in 'Mechanical Spectroscopy in Materials Science' (Ed. L. Magalas), Elsevier, Amsterdam, 1994
16 Camberlin, Y. and Pascault, J. P. *J. Polym. Sci. Chem.* 1989, **21**, 415
17 Etienne, S., Perez, P., Darud, V. and Pascault, J. P. *Makromol. Chem., Macromol. Symp.* 1989, **23**, 241
18 Perez, J., Etienne, S. and Tatibouet, J. *Phys. Status Solidi (a)* 1990, **121**, 129
19 Guinier, A. and Fournet, G., 'Small Angle Scattering of X-Rays', Wiley, New York, 1955
20 Koberstein, J. T., Morra, B. and Stein, R. S. *J. Appl. Crystallogr.* 1980, **13**, 34
21 Leung, L. M. and Koberstein, J. T. *J. Polym. Sci.* 1985, **23**, 1883
22 Martin, G. in 'Solid State Transformation in Metals and Alloys', Les Editions de Physique, Paris, 1978, pp. 337–406
23 Wagner, C. *Elektrochemie* 1961, **65**, 581
24 Bueche, R. 'Physical Properties of Polymers', Wiley-Interscience, New York, 1962
25 Bengston, B., Feger, C. and MacKnight, W. J. *Polymer* 1985, **26**, 895